

## ARTICLES

**Experimental and Theoretical Study of the XYO (X, Y = Cl, Br) Light-Induced Interconversion in Argon Matrix****P. Chaquin\****Laboratoire de Chimie Théorique, Unité propre du CNRS 9070, Université Pierre et Marie Curie, Tour 22, case 137, 4 place Jussieu, 75252 Paris Cedex 05, France***M. E. Alikhani***Laboratoire de Spectrochimie Moléculaire, Université Pierre et Marie Curie, Bat. F, 4 place Jussieu, 75252 Paris Cedex 05, France***M. Bahou, L. Schriver-Mazzuoli,<sup>‡</sup> and A. Schriver***Laboratoire de Physique Moléculaire et Applications,<sup>‡</sup> Unité propre du CNRS 136, Université Pierre et Marie Curie, Tour 13, case 76, 4 place Jussieu, 75252 Paris Cedex 05, France**Received: January 29, 1998; In Final Form: July 31, 1998*

The complex ClBrO has been generated in argon matrix by photolysis of the O<sub>3</sub>:BrCl complex and has been characterized by its Fourier-transform IR spectrum. Wavelength dependence of ClBrO photochemistry has been determined in the range from 317 to 870 nm by using laser irradiations and in the frequency region of a Nernst globar. Visible irradiation between 633 and 700 nm transforms ClBrO into BrClO and that above 700 nm continues the transformation into BrOCl. Reverse photoisomerization of BrOCl into ClBrO or BrClO was not observed. BrClO but not ClBrO is sensitive to IR irradiation. Calculations are combined with experimental observations to present a model for the photochemical isomerization of ClBrO and a comparison with related Cl<sub>2</sub>O and Br<sub>2</sub>O isomerizations.

**Introduction**

In a previous paper, studies of the photolysis of complexes between ozone and halogen molecules (Cl<sub>2</sub>, Br<sub>2</sub>, BrCl) were reported, using matrix isolation techniques.<sup>1</sup> Formation of BrBrO and ClBrO was observed after irradiation of the Br<sub>2</sub>:O<sub>3</sub> and ClBr:O<sub>3</sub> complexes, respectively, with 870-, 633-, and 532-nm laser lines. In the course of that work, isomerization of ClBrO into BrOCl and BrClO was observed as secondary pathways and initiated a further study of the spectra changes, which will be described here experimentally and theoretically.

Chlorine and bromine oxides are key species in ozone depletion in the stratosphere,<sup>2</sup> and an understanding of the selectivity of breaking a specific chemical bond in these species is of great interest. Although photoisomerization is less favorable in the gas phase than in condensed matter, it may play a role in the photochemistry of halogen oxides in cloud particles.<sup>3</sup> Some experimental studies of photoisomerization of halogen oxides have been carried out in matrixes. The symmetric OCIO is transformed into asymmetric ClOO by near-UV irradiation, and the reaction can be reversed by irradiation near 230 nm.<sup>4,5</sup> Maier and Bothur showed that BrOO undergoes

photoisomerization into OBrO upon irradiation at 254 nm,<sup>6</sup> whereas the photodestruction spectrum of OBrO into BrOO is a broad band starting at 400 nm and ending at 600 nm.<sup>7</sup> Recently, Johnson et al. reported a reverse-photoisomerization study of the compounds XOCIO (X = Cl, Br, I) prepared in argon matrix by addition of X to OCIO.<sup>8</sup> In the present work our interest concerns the interconversion of ClBrO isomers for which equilibrium structure, energy, and vibration frequencies have been recently determined by ab initio calculations.<sup>9,10</sup> Unfortunately, attempts to prepare ClBrO directly have remained unsuccessful and in this study, we prepared matrix-isolated ClBrO in situ by photolysis of the ClBr:O<sub>3</sub> complex at 532 nm as described earlier.<sup>1</sup> In the following, we describe the transformation of chlorine bromine oxide in argon matrix at selected wavelengths (from UV to IR radiation), having monitored the chemistry by means of absorption spectroscopy. Ab initio calculations on the possible dissociation dynamics are reported.

**Experimental Section**

**Matrix Isolation Studies.** The matrix isolation apparatus has been described previously.<sup>1</sup> ClBrO was prepared by photolysis of a Br<sub>2</sub>/Cl<sub>2</sub>/O<sub>3</sub>/Ar mixture (2/2/1/1000 by vol). Ozone was prepared from natural oxygen (Air Liquide N55) and <sup>18</sup>O<sub>2</sub> (Isotec) by silent electric discharge. Bromine (99%, supplied from Fluka) and chlorine (99.9%, supplied from

\* Author for correspondence. E-mail: chaquin@Lct.jussieu.fr.

<sup>†</sup> Also at Université Paris-Nord (Laboratoire de Recherche des Nuisances Atmosphériques).

<sup>‡</sup> Laboratoire Associé aux Universités P. et M. Curie et Paris-Sud.

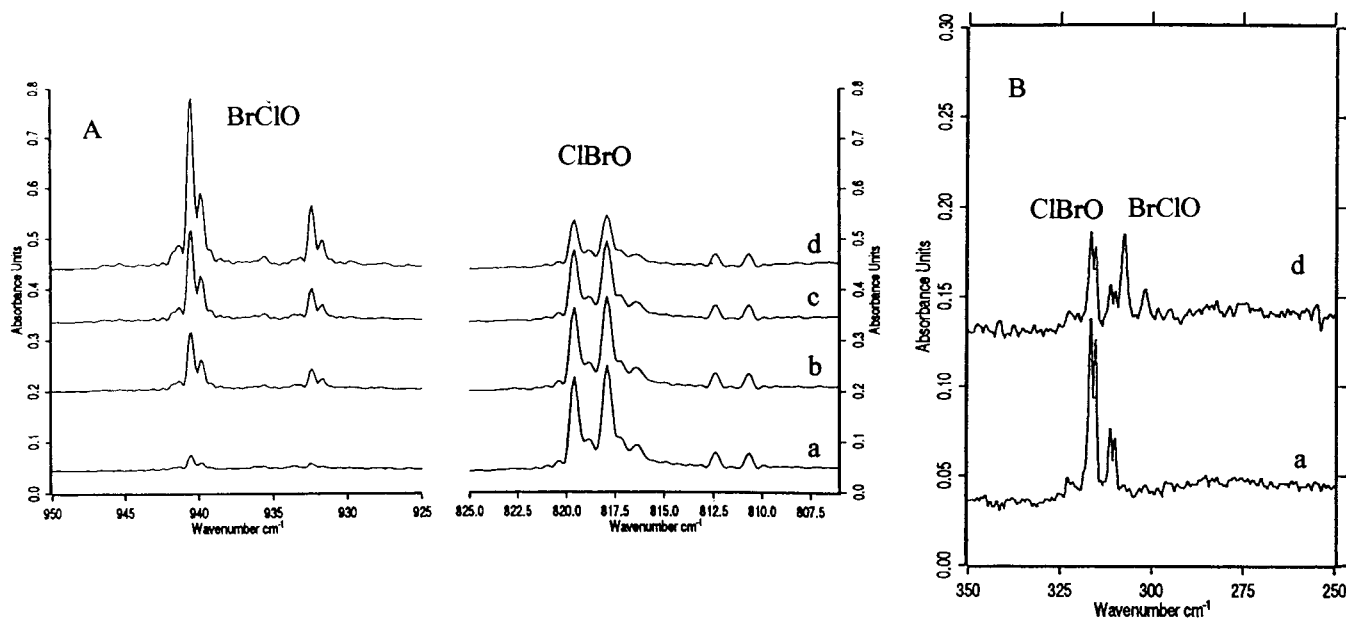


**Figure 1.** Comparison of the spectra in the 950–805  $\text{cm}^{-1}$  (A) and 350–250  $\text{cm}^{-1}$  (B) regions before irradiation (a) and after irradiation with the 532-nm laser line for 10 (b), 20 (c), and 60 min (d).

Matheson) were distilled in a vacuum. Argon (Air Liquide N56) was used without further purification. Deposition of the matrix was carried out in twin-jet mode, the halogen molecules and ozone in argon being deposited at 20 K from separate inlets. Irradiation at 10 K with the 532-nm laser line for 2 h with a flux of  $5 \times 10^{16}$  photons  $\text{cm}^{-2} \text{s}^{-1}$  led to disappearance of the  $\text{O}_3\text{:BrCl}$  and  $\text{O}_3\text{:Br}_2$  complexes and formation of  $\text{ClBrO}$  and  $\text{BrBrO}$  species. IR spectra were recorded with a Bruker 113v instrument in reflection mode between 4000 and 200  $\text{cm}^{-1}$  with a resolution of 0.5  $\text{cm}^{-1}$ . Irradiation was carried out with a 150 W Xe arc lamp, a Nernst globar, a home-built  $\text{CO}_2$  laser, and a TDL 50 dye laser pumped by a Nd:YAG laser YG 781C-20 (Quantel). Xenon-filtered light was obtained by using a filter RG715 (Schott),  $\lambda > 720$  nm.

**Calculation Methods.** The GAUSSIAN 94 series of programs<sup>11</sup> has been used throughout this work. Previous studies have shown<sup>9</sup> that density functional theory (DFT) methods afford good geometrical parameters and vibration frequencies in a series of halogen–oxygen compounds but often yield poorly reliable energies. Reliable energetic parameters require an extensive treatment of the correlation, for example, by the coupled cluster CCSD(T) method,<sup>10</sup> wasting computational time, with large basis sets. A good compromise is thus to calculate geometrical parameters at the DFT level and then to perform a single-point calculation at the CCSD(T) level. For zero-order stationary points, previously published<sup>9</sup> geometries have been used. Transition states (TS) have been optimized by using Becke's three-parameter functional<sup>12</sup> with correlation functional of Lee, Yang, and Parr<sup>13</sup> (B3-LYP) and checked by vibrational analysis. A basis set derived from Ahlrichs and colleagues<sup>14</sup> by adding 2d atomic orbitals (AOs) ( $\alpha_d = 2.314$  and 0.645) on oxygen and 2d AOs ( $\alpha_d = 1.072$  and 0.357) on chlorine has been used, yielding O, 11s 6p 2d/5s 3p 2d; Cl, 14s 8p 1d/5s 4p 2d; and Br, 17s 13p 6d/6s 5p 2d. At the CCSD(T) level, this basis set has been found to reproduce within  $\sim 2$  kcal  $\text{mol}^{-1}$  the relative energies calculated by Lee<sup>10</sup> for  $\text{ClBrO}$  isomers.

## Results and Discussion

**Experimental Studies.** *Infrared Spectrum of  $\text{ClBrO}$  Molecule in Argon Matrix.* Equilibrium structure, vibrational

frequencies, and energy of the  $\text{ClBrO}$  molecule as well as other  $\text{X}_2\text{O}$  and  $\text{XYO}$  species (X, Y = Cl, Br) have been recently determined by using DFT and ab initio calculations.<sup>9,10</sup>  $\text{ClBrO}$  has a short BrO bond ( $1.683 \pm 0.2$  Å) and a long BrCl bond ( $2.322 \pm 0.2$  Å) with an angle value of  $112.1^\circ \pm 0.5^\circ$ . Vibration frequencies were calculated at 808, 301, and 182  $\text{cm}^{-1}$ . Experimentally, we observed two IR bands. The first one, previously reported,<sup>1</sup> appeared as a doublet of equal components at 819.6 and 817.9  $\text{cm}^{-1}$  and was assigned to the BrO-stretching fundamental mode, the splitting being caused by natural isotope abundance ( $^{79}\text{Br}$ , 50.54%;  $^{81}\text{Br}$ , 49.6%). The second band was observed as two doublets at 315.5 and 310.1  $\text{cm}^{-1}$ , corresponding to the ClBr-stretching vibration for various chlorine isotopomers. Substitution of  $^{18}\text{O}$  in the  $\text{ClBrO}$  species resulted, as expected, in a shift of the 819.6–817.9  $\text{cm}^{-1}$  absorption to 780.1 and 778.9  $\text{cm}^{-1}$ , whereas the BrCl band was displaced only 0.2  $\text{cm}^{-1}$ . In the  $\nu_{\text{BrO}}$  region a weak doublet of equal components at 812.3–810.6  $\text{cm}^{-1}$ , which shifted to 774.5–772.6  $\text{cm}^{-1}$  when using  $^{18}\text{O}_3$ , was also observed after prolonged irradiation of the  $\text{ClBrO}:\text{O}_3$  complex. The doublet was not assigned.

**$\text{ClBrO} \rightarrow \text{BrClO}$  Transformation.** In Figure 1, trace (a) shows the spectrum of  $\text{ClBrO}/\text{Ar}$  recorded in the 950–805  $\text{cm}^{-1}$  (Figure 1A) and 350–250  $\text{cm}^{-1}$  (Figure 1B) region. Other traces are the corresponding spectra obtained after different irradiation times at 633 nm (photon flux =  $(2.1 \pm 0.2) \times 10^{16}$  photons  $\text{cm}^{-2} \text{s}^{-1}$ ). Note that the characteristic bands of the  $\text{ClBrO}$  species at 819.6–817.9  $\text{cm}^{-1}$  and at 316.8–311.4  $\text{cm}^{-1}$  decrease, while in parallel new doublets with relative intensity of their components of 3/1 appear at 940.5–932.4 and 307.6–301.9  $\text{cm}^{-1}$ . We have assigned these to the ClO and BrCl fundamental modes of the  $\text{BrClO}$  molecule, the splitting being due to natural chlorine isotopes. Figure 2 displays the intensity evolution of one characteristic band of each product versus photolysis time. At short times, the band at 940.5  $\text{cm}^{-1}$  grows rapidly without sigmoidal character. If we take into account that the absorption coefficient ratio for  $\nu_{\text{BrO}}$  and  $\nu_{\text{ClO}}$  stretches is  $\sim 2.0 \pm 0.2$ , the disappearance of  $\text{ClBrO}$  is nearly correlated to the growth of  $\text{BrClO}$ . At long irradiation times,  $\text{ClBrO}$  disappears totally and the  $\nu_{\text{ClO}}$  intensity approaches a constant value. Experimental curves relative to the 819.6  $\text{cm}^{-1}$  disap-

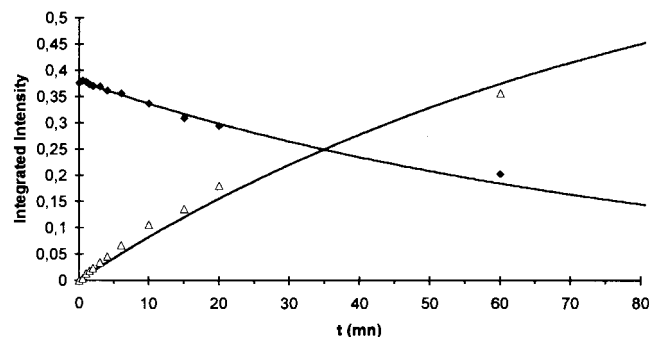


**Figure 2.** Decay curve of ClBrO species and growth curve of BrClO species during photolysis with the 633-nm laser line. For comparison, integrated intensity of the  $\nu_{\text{BrO}}$  absorption of ClBrO was multiplied by 2.5 (see text).

pearance and the  $940.5\text{ cm}^{-1}$  growth were well fitted by the first-order relationships  $A^0_{\text{BrO}} \exp(-kt)$  and  $A^\infty_{\text{ClO}} (1 - \exp(-kt))$ , respectively, where the quantities  $A^0$  and  $A^\infty$  are the initial integrated intensity of the BrO band and the asymptotic limit of the BrClO growth curve, respectively. In the given experiment, with a photon flux  $= (2.1 \pm 0.2) \times 10^{16}$  photons  $\text{cm}^{-2}$   $\text{s}^{-1}$ , the rate coefficient  $k$  was found to be  $(1.8 \pm 0.1) \times 10^{-4}$   $\text{s}^{-1}$ ; unfortunately, however, in the absence of knowledge of the absorption cross-section for the visible absorption bands,

we were unable to calculate the quantum yield of the isomerization. Transformation of ClBrO into BrClO was also observed after irradiation with the 693-nm laser line, but with a filtered xenon lamp ( $\lambda > 720$  nm), only the transformation of ClBrO into BrOCl occurred, as reported below.

Attempts to observe the back-isomerization of BrClO into ClBrO by using visible wavelengths remained unsuccessful. However, in the UV region, as illustrated in Figure 3A, the BrClO species decreased with the 317-nm laser line, whereas ClBrO appeared. The reverse-transformation was also observed (Figure 3B) from ClBrO. In both cases, a stationary state between ClBrO and BrClO was reached after 10 min of 317-nm irradiation.

*ClBrO  $\rightarrow$  BrOCl Transformation: Irradiation in the Visible Region.* Irradiation of matrix-isolated ClBrO with the filtered xenon lamp ( $\lambda > 720$  nm) or with the 870-nm laser line transformed ClBrO into BrOCl, as was identified by absorptions located at  $675.9$  and  $559.5\text{ cm}^{-1}$ . They appeared in addition to the characteristic absorptions of BrOBr produced from BrBrO transformation. When isotopic ClBr $^{18}\text{O}$  species were irradiated, they were shifted to  $648.5$  and  $533.4\text{ cm}^{-1}$ , respectively, as displayed Figure 4. These absorptions are assigned to the ClO- and BrO-stretching fundamentals.

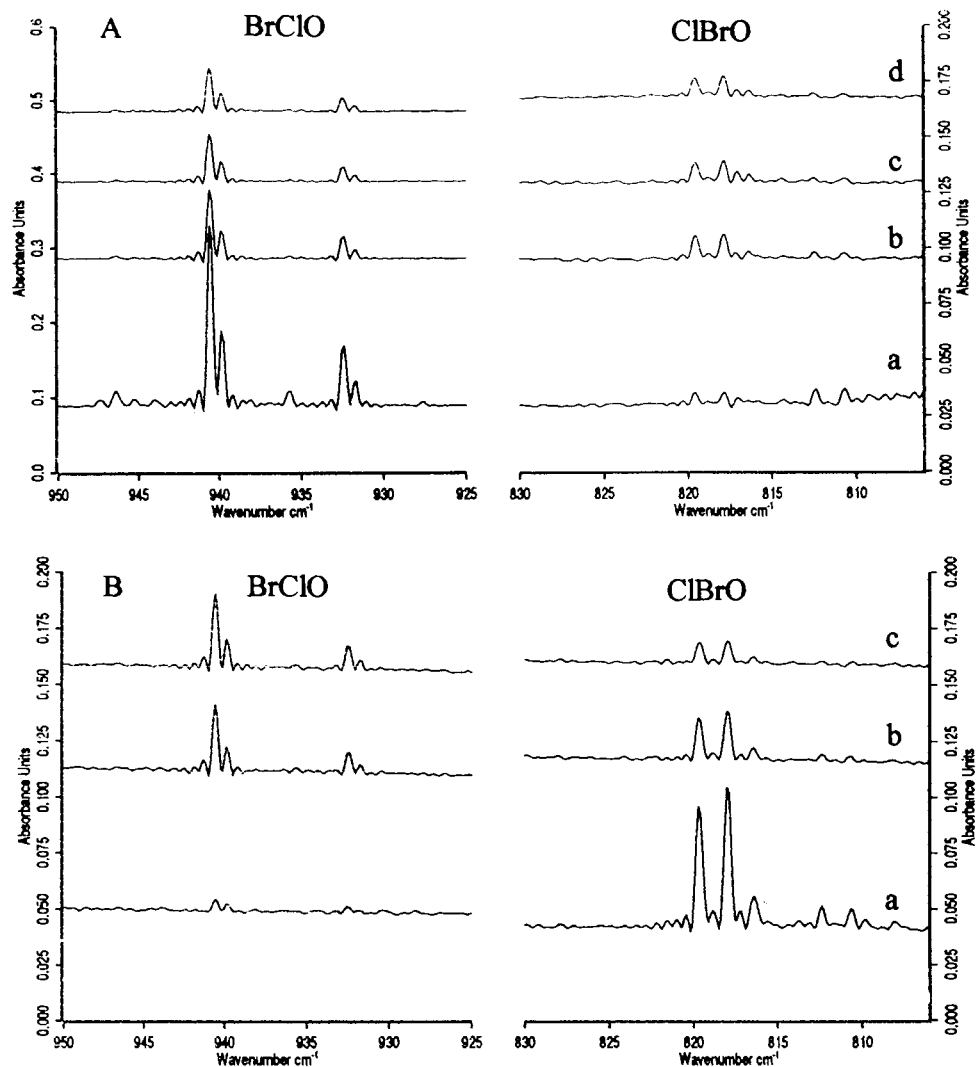


**Figure 3.** Evolution of the spectrum of BrClO (A) and ClBrO (B) species in the  $\nu_{\text{NO}}$  region after irradiation at 10 K with the  $\lambda = 317$ -nm laser line. Irradiation times (minutes) in A: (a) 0, (b) 10, (c) 20, (d) 60; in B: (a') 0, (b') 10, (c') 20.

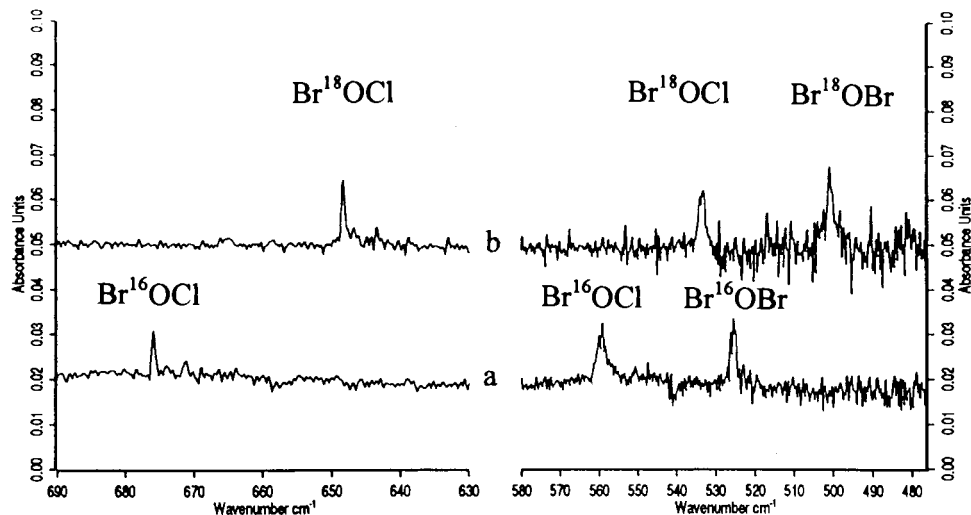


**Figure 4.**  $\nu_{\text{ClO}}$  and  $\nu_{\text{BrO}}$  regions in the spectra of  $\text{Br}^{16}\text{OCl}$  (a) and  $\text{Br}^{18}\text{OCl}$  (b) species generated in matrixes by irradiation of  $\text{ClBrO}$  with a filtered xenon lamp ( $\lambda > 720$  nm).

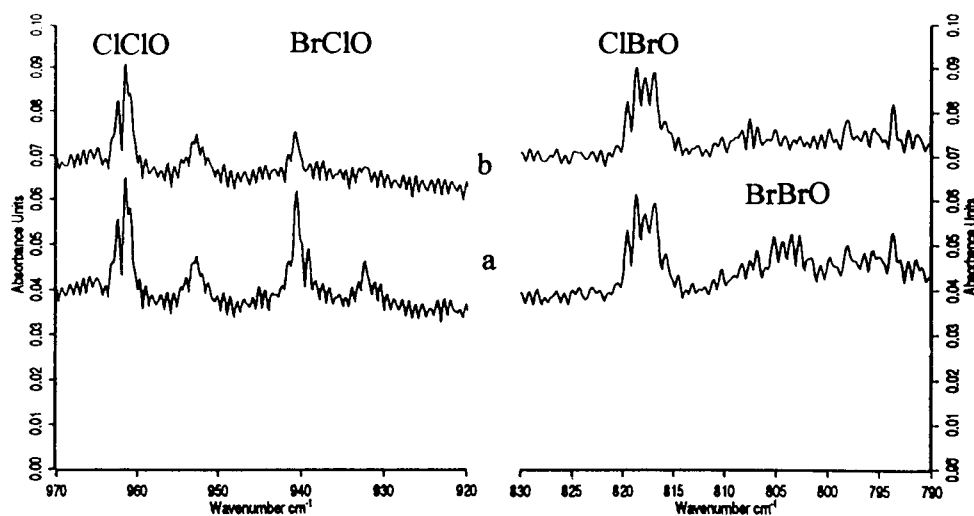


**Figure 5.** Spectral changes observed after irradiation with Nernst globar (120 min) for  $\text{ClClO}$ ,  $\text{BrClO}$ ,  $\text{ClBrO}$ , and  $\text{BrBrO}$  in the  $\nu_{\text{XO}}$  ( $X = \text{Cl, Br}$ ) mode region. (a) Before and (b) after irradiation.

When  $\text{BrClO}$  was irradiated at 870 nm, it too was transformed into  $\text{BrOCl}$ . No back-transformation of  $\text{XOX}$  ( $X = \text{Br, Cl}$ ) into  $\text{XXO}$  species was observed in the wavelength range 317–870  $\text{cm}^{-1}$ .

Table 1 summarizes all the observed frequencies in this work and their assignment.

**Infrared-Induced Photodecomposition.** Tevault et al.,<sup>15</sup> and then Allen et al.,<sup>16</sup> reported that the  $\text{BrBrO}$  species was converted into  $\text{BrOBr}$  by Nernst globar irradiation. To observe the possible formation of  $\text{BrOCl}$  by IR irradiation, we first irradiated an  $\text{O}_3/\text{Br}_2$ ,  $\text{Cl}_2/\text{Ar}$  mixture with the full output light of the xenon lamp for 1 h and followed this by annealing to produce  $\text{ClClO}$ ,  $\text{BrClO}$ ,  $\text{ClBrO}$ , and  $\text{BrBrO}$  as described previously;<sup>17</sup> we then irradiated the mixture with the Nernst globar (1–50  $\mu\text{m}$  range) for 120 min. As illustrated in Figure 5, absorptions at 805.4 and 940.5  $\text{cm}^{-1}$ , characterizing the  $\text{BrBrO}$  and  $\text{BrClO}$  species, strongly diminished, whereas the intensities of the 961  $\text{cm}^{-1}$  ( $\text{ClClO}$ ) and 819.6  $\text{cm}^{-1}$  ( $\text{ClBrO}$ ) absorptions remained unchanged. Irradiation with the  $\text{CO}_2$  laser line emission (of the transition  $00^0_1 \rightarrow 10^0_0$ ) at 940.54  $\text{cm}^{-1}$  (P24) at the same frequency as the  $\nu_{\text{ClO}}$ -stretching mode of  $\text{BrClO}$  led also to the decrease of the  $\text{BrClO}$  absorption at 940.5  $\text{cm}^{-1}$  as displayed in Figure 6, indicating an efficient selective excitation of the  $\nu_{\text{ClO}}$  mode. However, no new bands were

**TABLE 1: Characteristic Vibration Frequencies ( $\text{cm}^{-1}$ ) of  $\text{ClBrO}$ ,  $\text{BrClO}$ , and  $\text{BrOCl}$  Species Trapped in Argon Matrix**

	$\text{ClBrO}$		$\text{BrClO}$		$\text{BrOCl}$	
	$^{16}\text{O}$	$^{18}\text{O}$	$^{16}\text{O}$	$^{18}\text{O}$	$^{16}\text{O}$	$^{18}\text{O}$
$\nu_3$	819.6	780.1	940.5	905.2	675.9	648.5
	817.9	778.9	932.4	896.5	671.2	643.6
$\nu_2$	316.8–315.5	316.4–315.2	307.6		559.5	533.4
	311.4–310.1	310.9–309.8	301.9			

observed in all the spectral range, and the  $\text{BrBrO}$  photodecomposition did not lead to the  $\text{BrOBr}$  species as had been previously reported. Indeed, isomerization of isolated  $\text{BrBrO}$  into  $\text{BrOBr}$  involves a process in which a bond is broken and hence requires an activation energy superior to the energy given by single IR-selective photoabsorption. Only photodissociation of weak hydrogen-bonded complexes or conformational isomerizations produced by selective irradiation, and some additional reactions of unstable molecules, have been described with certitude in matrixes.<sup>18–20</sup> The absence of new IR absorption bands and the lack of variation in intensity of  $\text{BrCl}$  and ozone in our experiments after disappearance of  $\text{BrClO}$ , as well as the different behaviors of  $\text{ClBrO}$  and  $\text{BrClO}$  after IR irradiation, are not straightforward to explain, and we cannot exclude the

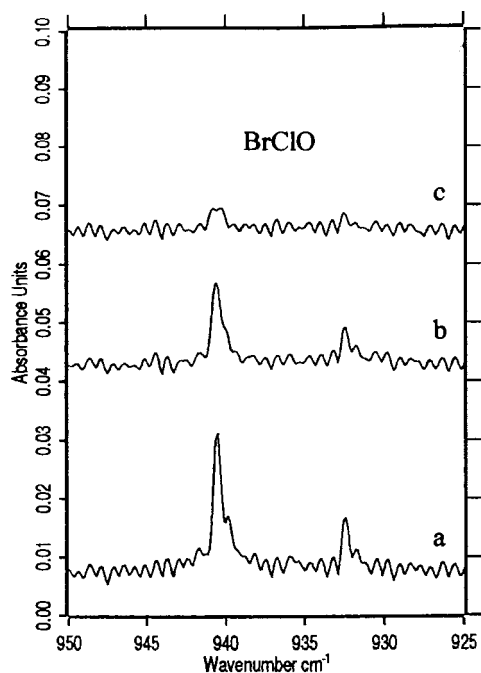


**Figure 6.** FTIR spectra recorded in the  $\nu_{\text{ClO}}$  region of BrClO species (a) before irradiation; (b) after irradiation with a CO<sub>2</sub> laser line (transition 00<sup>0</sup>1 → 10<sup>0</sup>0) at 940.54 cm<sup>-1</sup> (P<sub>24</sub>) for 45 min; and (c) after irradiation of (b) with Nernst globar for 110 min.

possibility that these observations could be effects of partial vaporization of the matrix.

**Theoretical Study.** *Interconversions of ClBrO Species.* The electronic ground-state (GS) energy profiles of the following interconversion reactions are displayed in Figure 7; the corresponding energies are reported in Table 2:



The calculated geometry, relative energy, and vibration frequencies of the reactants have been already discussed.<sup>9,10</sup> The optimized geometries at the DFT (B3-LYP) level are recalled in parentheses in Figure 8. Lee,<sup>10</sup> at the CCSD(T) level and using very large basis sets, concluded that ClBrO lies ~18.5 kcal mol<sup>-1</sup> above ClOBr and 6.7 kcal mol<sup>-1</sup> under BrClO. The TS geometries are displayed in Figure 7.

The attribution of each TS to the corresponding process has been made with the help of the normal mode associated with the imaginary frequency. Examination of their geometrical parameters supports this attribution. In all cases, the migrating atom exhibits rather long distances from the other two atoms, the latter atoms having a bond length very close to (and even slightly shorter than) that of the isolated diatomic species, calculated at the same level and given in parentheses: 2.17 Å for Br–Cl in TS1 (2.21 Å), 1.71 Å for Br–O in TS2 (1.77 Å), and 1.58 Å for Cl–O in TS3 (1.62 Å).

Reaction 2 needs an activation energy of 24.8 kcal mol<sup>-1</sup> (zero-point energy (ZPE) correction  $-5 \times 10^{-4}$  au), and reaction 3 needs 12.3 kcal mol<sup>-1</sup> (ZPE correction  $-6 \times 10^{-4}$  au). These values reflect the relative weakness of the Br–Cl bond, which is partially broken in the TS. Reaction 1 exhibits an unexpected activation energy of nearly 70 kcal mol<sup>-1</sup>, which is higher than the energy of the bond, ClO or BrO, to be broken, ~52 or 48 kcal mol<sup>-1</sup>, respectively. One can remark that TS2 and TS3

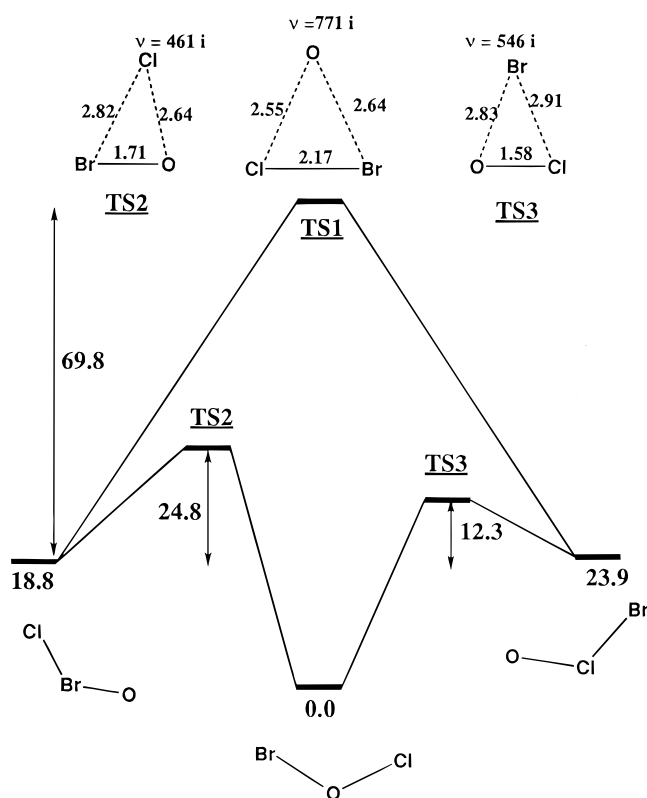


**Figure 7.** ClBrO isomerizations. Calculated reaction profiles (energies in kcal mol<sup>-1</sup>, geometry (distances in Å), and imaginary frequency (cm<sup>-1</sup>) of TS1, TS2, and TS3 transition states.

**TABLE 2: Stationary Point Energy in ClBrO Potential Energy Surface (See Also Figure 7)**

	CCSD <sup>a</sup>	CCSD(T) <sup>a</sup>	ZPE <sup>b</sup>	$\Delta E^c$
ClBrO <sup>d</sup>	0.19517	0.22252	2.7	18.8
TS1	0.09288	0.11127	1.4	88.6
BrClO <sup>d</sup>	0.18961	0.21418	3.0	23.9
TS2	0.10480	0.18303	2.2	43.6
BrOCl <sup>d</sup>	0.23114	0.25245	3.1	0.0
TS3	0.14824	0.19452	2.4	36.2

<sup>a</sup>  $-(3107 + E)$  au. <sup>b</sup> Calculated from B3-LYP frequencies,  $\times 10^3$  au. <sup>c</sup> Reaction energies (kcal mol<sup>-1</sup>) with respect to ClBrO, at the CCSD(T) level. <sup>d</sup> B3-LYP geometry taken from ref 9.

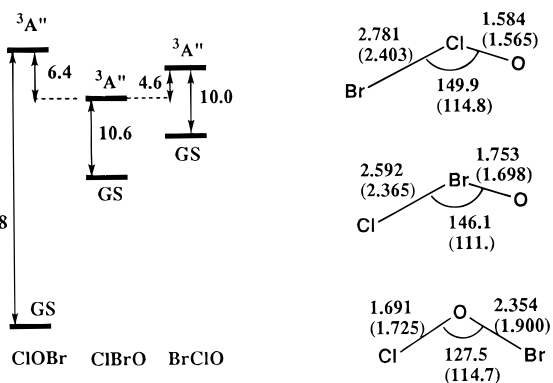


**Figure 8.** CCSD(T)/B3-LYP triplet energy (kcal mol<sup>-1</sup>) with respect to GS and triplet-optimized geometries (B3-LYP) of ClOBr, ClBrO, and BrOCl (bond lengths in Å, angles in deg; GS parameters taken from Chaquin et al.<sup>9</sup>).

resemble a XO<sup>0</sup>–Y<sup>0</sup> radical pair, the ground state of which at infinite separation is singlet or triplet XO<sup>0</sup> plus Y<sup>0</sup>. In contrast, TS1 looks like a ClBr–O molecule–atom complex whose GS



is triplet (singlet BrCl plus triplet O). Thus the lowest singlet state  $^1A'$  of this system, correlated to ClBr (GS) plus excited O ( $^1D$ ) at infinite separation, appears as an excited state lying  $\sim 50$  kcal mol $^{-1}$  ( $^1D$ - $^3P$  gap in oxygen atom) above the GS.

Only CCSD(T) activation energies will be used in further discussion, since DFT, in some cases, has been found to underestimate energy barriers, though it is suitable in other cases (e.g., Diels–Alder reactions<sup>21</sup>). In the present work, B3LYP activation energies are rather close to the CCSD(T) ones and do not appear to systematically over- or underestimate these data: for reaction 1, the barrier is found to be lower by 2.3 kcal mol $^{-1}$ , and for reactions 2 and 3, the barriers are higher by 3.7 and 2.3 kcal mol $^{-1}$ , respectively.

Another possibility for ClBrO isomerizations is an evolution of the system on an excited (singlet or triplet) potential energy surface (PES). We thus performed, as a first step, qualitative calculation of vertical singlet-excitation energies, using the configuration interaction using single excitations (CIS) method.

BrClO  $^1A''$ : 700 nm (41 kcal mol $^{-1}$ ), forbidden

$2^1A'$ : 420 nm (68 kcal mol $^{-1}$ ), weak

$2^1A''$ : 385 nm (74 kcal mol $^{-1}$ ), forbidden

$3^1A'$ : 268 nm (106 kcal mol $^{-1}$ ), strong

ClBrO  $^1A''$ : 560 nm (51 kcal mol $^{-1}$ ), forbidden

$2^1A'$ : 311 nm (92 kcal mol $^{-1}$ ), weak

$2^1A''$ : 305 nm (94 kcal mol $^{-1}$ ), forbidden

$3^1A'$ : 274 nm (104 kcal mol $^{-1}$ ), strong

BrOCl  $^1A''$ : 365 nm (78 kcal mol $^{-1}$ ), weak

$2^1A'$ : 281 nm (101 kcal mol $^{-1}$ ), weak

These results are expected to be poorly reliable, and probably overestimated, but provide qualitative differences in the absorption spectra. Compared with high-level calculations performed on ClOCl and ClClO,<sup>22</sup> the overestimation is in the range 0.5–1 eV.

The dominant configuration in the  $^1A''$  lowest-excited state results from the moving of one electron from the  $\pi^*$  ( $a''$ ) highest occupied molecular orbital (HOMO) of ClBrO and ClOBr and HOMO-1 of BrClO, of the same structure as  $\pi_3$  of ozone, into the  $\sigma^*$  ( $a'$ ) lowest unoccupied MO (LUMO). The latter MO is delocalized over both bonds in BrOCl, whereas this  $\sigma^*$  MO is mainly localized on Cl–Br in the other two species. Since this bond is weak, the corresponding  $\sigma^*$  MO is low in energy and is the reason the excitation energy is much lower for ClBrO and BrClO than for BrOCl. Moreover, this bond appears weaker (2.40 Å) in BrClO than in ClBrO (2.36 Å), in qualitative agreement with respective excitation energies. Other lowest-excited states of ClBrO and BrClO ( $2^1A'$  and  $2^1A''$ ) mainly involve the population of the same  $\sigma^*$  MO, antibonding along Cl–Br with an increasing participation of the LUMO + 1, which is strongly antibonding along Br–O and Cl–O, respectively. In contrast, the  $3^1A'$  of both species' excited state concerns essentially the LUMO + 1.

Lowest-triplet states have been examined at a higher calculation level. As a matter of fact, we can expect that the presence of bromine favors  $S_1 \rightarrow T_1$  interconversion. Furthermore, if

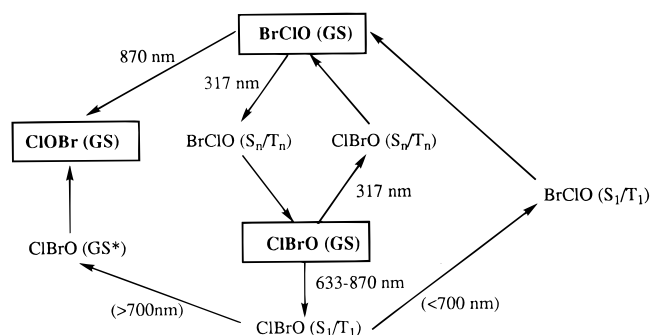


Figure 9. Tentative reaction scheme for ClBrO interconversions.

we consider a possible reaction along the open-shell singlet  $S_1$  PES, we would expect that for any case  $S_1$  and  $T_1$  PES values are almost parallel. Lowest-triplet ( $^3A''$ ) geometries have been optimized at the DFT level and their energies calculated at the CCSD(T) level (Figure 8). These states have roughly the same dominant configuration as  $^1A''$  singlets, with a significant increase of the Cl–Br bond lengths in ClBrO and BrClO, whereas the ClO and BrO bond lengths are less changed. Given these data, we cannot easily rationalize the experimental features. Nevertheless, several remarks can be made, leading to the possible reaction scheme of the Figure 9.

(1) The existence of a photostationary equilibrium BrClO–ClBrO upon irradiation at 317 nm is consistent with the fact that both of these species should absorb light strongly in this region, leading to an excited state that selectively weakens the halogen–oxygen bond. Indeed, at this wavelength, the system gets so much energy ( $\sim 100$  kcal mol $^{-1}$ ) that many other processes are likely to occur.

(2) The lack of reactivity of BrClO in the range 633–890 nm can be understood if we assume that the calculated absorption wavelength (700 nm) is overestimated by at least 0.5–1 eV and that the actual value could be shifted up to 1200–1500 nm.

(3) The BrClO  $\rightarrow$  BrOCl transformation at  $\lambda = 870$  nm can occur a priori either by an excited-state  $T_1$  or  $S_1$  reaction, since these states seem to induce a Cl–Br breaking, or by a “hot” GS isomerization. In fact, the excitation is energetic enough (35 kcal mol $^{-1}$ ) to reach **TS3**, but not **TS1**, which would yield ClBrO.

(4) The sensitivity of BrClO to 940 cm $^{-1}$  IR irradiation, which brings only  $\sim 3$  kcal mol $^{-1}$ , remains difficult to explain by a unimolecular cleavage or isomerization of this species.

(5) The most puzzling phenomenon is the selective transformation of ClBrO into BrClO between 633 and 700 nm. From the calculated absorption wavelengths, and taking into account the fact that these are probably overestimated, one can only assume that ClBrO absorbs light significantly in this region. Photon energy cannot ensure the overcoming of **TS1**, and thus a GS reaction should give BrOCl through **TS2** rather than BrClO. A first possibility is a  $T_1$  or  $S_1$  reaction: from Figure 8, we can see that the ClBrO ( $T_1$ )  $\rightarrow$  BrClO ( $T_1$ ) reaction is less endothermic than ClBrO ( $T_1$ )  $\rightarrow$  ClOBr ( $T_1$ ) and thus could be faster, although, as previously seen, the excitation preferentially weakens the Cl–Br bond. To support this hypothesis, calculation of the TS energies for these  $T_1$  PES values should be necessary. Unfortunately, criteria for convergence could not be met in optimizing the geometry of these TS, which, like the singlet ones, resemble a molecule–atom pair. As a matter of fact, the PES values are very flat, and a significant displacement of the migrating atom results in weak energy changes. Approximate energy barriers,  $E^*$ , for reactions 1–3 can neverthe-

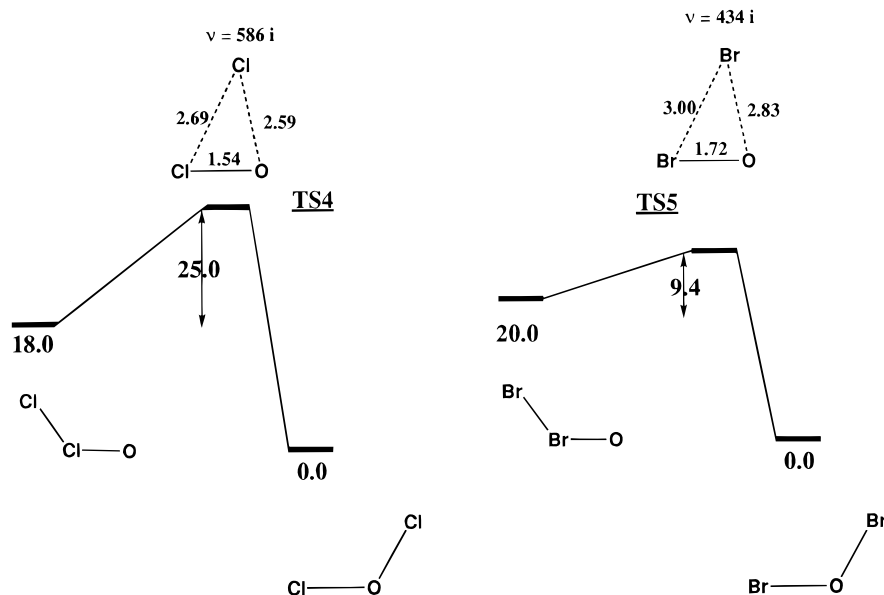
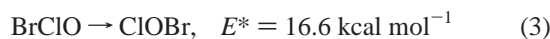
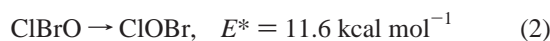
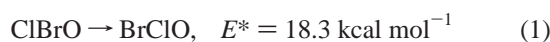


**Figure 10.**  $\text{Cl}_2\text{O}$  and  $\text{Br}_2\text{O}$  isomerization. Calculated reaction profiles (energies in  $\text{kcal mol}^{-1}$ ), geometry (distances in Å), and imaginary frequency ( $\text{cm}^{-1}$ ) of **TS4** and **TS5** transition states.

less be estimated at the CCSD(T) level:



Although we must consider these data with some caution, given the uncertainty in the geometrical parameters, reaction 2 again seems to be favored over reaction 1. The triplet TS for reaction 1 lies  $\sim 45 \text{ kcal mol}^{-1}$  below singlet **TS1**, which appears as an excited state of a triplet GS, as previously noted. Regarding the possibility of reaction on the open-shell singlet surface of the same configuration, we can assume that this surface is roughly parallel to that of the triplet and that reaction 2 should be favored.

Another possibility is that the  $\text{ClBrO} \rightarrow \text{BrClO}$  reaction is a bimolecular process. The only partner present in matrix sites in a significant amount is  $\text{O}_2$ , the byproduct of ozone photolysis. We can suppose, for instance, that triplet  $\text{ClBrO}$  plus triplet dioxygen yields an energy-rich  $\text{Cl-O-O-OB}_r$  intermediate, which can either give back  $\text{ClBrO}$  or evolve toward  $\text{BrClO}$  (plus  $\text{O}_2$ ); the latter increases since it does not absorb light.

(6) At longer wavelengths ( $\lambda > 700 \text{ nm}$ ),  $\text{ClBrO}$  presumably does not possess enough internal energy to yield  $\text{BrClO}$ , whatever the mechanism of this transformation. Thus, after deactivation, its only possibility is to yield  $\text{ClOBr}$  by way of a “hot” ground state, which needs  $24.8 \text{ kcal mol}^{-1}$ , or, less probably, by a hot  $T_1$  state, which needs  $\sim 12 \text{ kcal mol}^{-1}$  (see point 5).

*$\text{Cl}_2\text{O}$  and  $\text{Br}_2\text{O}$  Isomerizations.* Reaction profiles of isomerization reactions



are displayed in Figure 10. The corresponding absolute energies are reported in Tables 3 and 4. The energy difference between  $\text{ClClO}$  and  $\text{ClOCl}$  ( $18 \text{ kcal mol}^{-1}$ ) is very close to that reported by Lee<sup>10</sup> at the CCSD(T)/ANO-4 level ( $19 \text{ kcal mol}^{-1}$ ). The

**TABLE 3: Stationary Point Energy in  $\text{Cl}_2\text{O}$  Potential Energy Surface (See Also Figure 10)**

	CCSD <sup>a</sup>	CCSD(T) <sup>a</sup>	ZPE <sup>b</sup>	$\Delta E^c$
$\text{ClClO}^d$	0.37636	0.41208	3.7	18.0
<b>TS4</b>	0.31918	0.37237	2.7	43.0
$\text{ClOCl}^d$	0.41118	0.44089	3.5	0.0

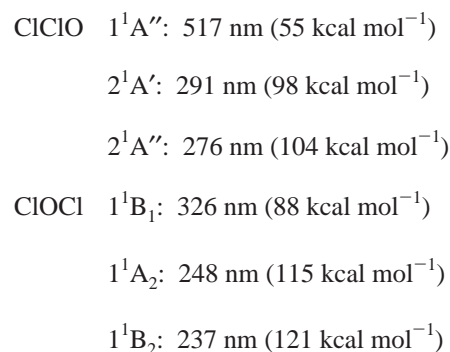
<sup>a</sup>  $-(994 + E)$  au. <sup>b</sup> Calculated from B3-LYP frequencies,  $\times 10^3$  au. <sup>c</sup> Reaction energies ( $\text{kcal mol}^{-1}$ ) with respect to  $\text{ClOCl}$ , at the CCSD(T) level. <sup>d</sup> B3-LYP geometry taken from ref 9.

**TABLE 4: Stationary Point Energy in  $\text{Br}_2\text{O}$  Potential Energy Surface (See Also Figure 10)**

	CCSD <sup>a</sup>	CCSD(T) <sup>a</sup>	ZPE <sup>b</sup>	$\Delta E^c$
$\text{BrBrO}^d$	0.08775	0.11484	2.5	20.0
<b>TS5</b>	0.05920	0.09990	2.0	29.4
$\text{BrOBr}^d$	0.12300	0.14674	3.0	0.0

<sup>a</sup>  $-(5220 + E)$  au. <sup>b</sup> Calculated from B3-LYP frequencies,  $\times 10^3$  au. <sup>c</sup> Reaction energies ( $\text{kcal mol}^{-1}$ ) with respect to  $\text{BrOBr}$ , at the CCSD(T) level. <sup>d</sup> B3-LYP geometry taken from ref 9.

semiquantitative vertical absorption wavelengths, calculated as for the  $\text{ClBrO}$  isomers, are as follows:



Comparison with the EOM-CCSD(T) calculations by Del Bene et al.<sup>22</sup> shows that these energy values are overestimated by  $> 1 \text{ eV}$  for the lower states to  $0.5 \text{ eV}$  for the upper states. According to these authors, the  $\text{GS} \rightarrow 1^1A''$  transition of  $\text{ClClO}$  is shifted into the near-IR (1143 nm), and the  $\text{GS} \rightarrow 1^1B_1$

transition for ClOCl is shifted to 493 nm. The calculated TS4 energy suggests that ClClO  $\rightarrow$  ClOCl could occur after near-IR irradiation, whereas the reverse transformation should require wavelengths shorter than  $\sim$ 650 nm. This qualitatively agrees with the existence under irradiation at 320–428 nm of a ClOCl–ClClO photostationary state.<sup>23</sup>

We found the energy difference between BrBrO and BrOBr to be 20 kcal mol<sup>-1</sup>, significantly greater than the 16.1 kcal mol<sup>-1</sup> reported by Lee.<sup>10</sup>

The activation energy for reaction 5 is weak, 9.4 kcal mol<sup>-1</sup> (8.9 kcal mol<sup>-1</sup> after ZPE correction). This suggests, nevertheless, that an IR photon at 940 cm<sup>-1</sup> is not energetic enough ( $\sim$ 3 kcal mol<sup>-1</sup>) to ensure overcoming the activation barrier. Absorption bands of BrBrO (1<sup>1</sup>A'', 706 nm; 2<sup>1</sup>A', 413 nm; 2<sup>1</sup>A'', 381 nm; 3<sup>1</sup>A', 288 nm) and of BrOBr (1<sup>1</sup>B<sub>1</sub>, 381 nm; 1<sup>1</sup>B<sub>2</sub> and 1<sup>1</sup>A<sub>2</sub>, 281 nm), at the CIS level, appear very similar to those of the couple ClClO–ClOCl, with a shift toward long wavelengths.

**Acknowledgment.** Computations were performed on an RS6000 workstation at the Institut de Développement des Ressources Informatiques Scientifiques (IDRIS, Orsay, France).

## References and Notes

- (1) Bahou, M.; Schriver-Mazzuoli, L.; Schriver, A.; Chaquin, P. *Chem. Phys.* **1997**, *216*, 105.
- (2) Wayne, R. P.; Poulet, G.; Biggs, P.; Burrows, J. P.; Cox, R. A.; Crutzen, P. J.; Hayman, G. O.; Jenkin, E.; Lebras, G.; Moortgat, G. K.; Platt, U.; Schindler, R. N. *Halogen Oxides: Radicals, Sources and Reservoirs in the Laboratory and in the Atmosphere*; European Commission Office for Official Publications of the European Communities: Luxembourg, 1995.
- (3) Purcell, C. *J. Phys. Chem.* **1995**, *99*, 10433.
- (4) Arkell, A.; Schwager, J. *J. Am. Chem. Soc.* **1967**, *89*, 599.

- (5) Johnson, K.; Engdahl, A.; Nelander, B. *J. Phys. Chem.* **1993**, *97*, 9603.
- (6) Maier, G.; Bothur, A. *Anorg. Z. Allg. Chem.* **1995**, 621, 743.
- (7) Kölm, J.; Engdahl, A.; Schrems, O.; Nelander, B. *Chem. Phys.* **1997**, *214*, 213.
- (8) Johnson, K.; Engdahl, A.; Kölm, J.; Nieminen, J.; Nelander, B. *J. Phys. Chem.* **1995**, *99*, 3902.
- (9) Chaquin, P.; Bahou, M.; Schriver-Mazzuoli, L.; Schriver, A. *Chem. Phys. Lett.* **1996**, *256*, 609.
- (10) Lee, T. J. *J. Phys. Chem.* **1995**, *99*, 15074.
- (11) Frisch, M. J.; Trucks, G. W.; Schlegel, H. B.; Gill, P. M. W.; Johnson, B. G.; Robb, M. A.; Cheeseman, J. R.; Keith, T.; Petersson, G. A.; Montgomery, J. A.; Raghavachari, K.; Al-Laham, M. A.; Zakrzewski, V. G.; Ortiz, J. V.; Foresman, J. B.; Cioslowski, J.; Stefanov, B. B.; Nanayakkara, A.; Challacombe, M.; Peng, C. Y.; Ayala, P. Y.; Chen, W.; Wong, M. W.; Andres, J. L.; Replogle, E. S.; Gomperts, R.; Martin, R. L.; Fox, D. J.; Binkley, J. S.; Defrees, D. J.; Baker, J.; Stewart, J.; Head-Gordon, M.; Gonzalez, C.; Pople, J. A. *GAUSSIAN 94*, Revision B.1; Gaussian Inc.: Pittsburgh, PA, 1995.
- (12) Becke, A. D. *J. Chem. Phys.* **1993**, *98*, 5648.
- (13) Lee, C.; Yang, W.; Paar, R. G. *Phys. Rev.* **1988**, *B37*, 785. Mielich, B.; Savin, A.; Stall, H.; Preuss, H. *Chem. Phys. Lett.* **1989**, *157*, 200.
- (14) Schaefer, A.; Huber, C.; Ahlrichs, R. *J. Chem. Phys.* **1994**, *100*, 5829.
- (15) Tevault, D. E.; Walker, N.; Smardzewski, R. R.; Fox, W. B. *J. Phys. Chem.* **1978**, *82*, 2733.
- (16) Allen, S. D.; Poliakov, M.; Turner, J. J. *J. Mol. Struct.* **1987**, *157*, 1.
- (17) Schriver-Mazzuoli, L.; Abdelaoui, O.; Lugez, C.; Schriver, A. *Chem. Phys. Lett.* **1993**, *214*, 519.
- (18) Frei, H.; Pimentel, G. C. *Annu. Rev. Phys. Chem.* **1985**, *36*, 491.
- (19) Barnes, A. J. *J. Mol. Struct.* **1984**, *113*, 161.
- (20) Schriver-Mazzuoli, L.; Schriver, A.; Perchard, J. P. *J. Mol. Struct.* **1990**, *222*, 141.
- (21) Goldstein, E.; Beno, B.; Houk, K. N. *J. Am. Chem. Soc.* **1996**, *118*, 6036.
- (22) Del Bene, J. E.; Watts, J. D.; Barlett, R. J. *Chem. Phys. Lett.* **1995**, *246*, 541.
- (23) Johnson, K.; Engdahl, A.; Nelander, B. *J. Phys. Chem.* **1995**, *99*, 3965.